

Adsorption Kinetic, Thermodynamic Studies for the Removal of Methylene Blue from Aqueous Solution using Modified Variegated Sky Flower Stem

Ajaelu C. J.^{1*}, Alabi S.¹ and Ikotun A. A.¹

¹Industrial Chemistry Programme, College of Agriculture, Engineering and Science, Bowen University, Iwo, Nigeria

*Corresponding Author: chijioke.ajaelu@bowen.edu.ng

Abstract

Wastewater from dye-producing factories contaminates water bodies leading to deleterious effects on man, plants and animals. This study investigated the performance of citric acid-modified Variegated Skyflower stem powder (MVSF) in the methylene blue (MB) removal from aqueous solution. Adsorbent morphological characterization and functional group determination were carried out using Scanning Electron Microscopy (SEM) and Fourier Transform Infrared spectrometer (FTIR). The batch adsorption experiments carried out included pH, temperature effect, contact time and initial dye concentration. The optimum pH of sorption was 5.0. The maximum sorption capacity for the adsorption of MB was 107.5 mg/g. Freundlich ($R^2 = 0.996$) and Dubini-Raduchkevich D-R ($R^2 = 0.992$) models gave the best fit for the adsorption of MB by modified Variegated Sky Flower stem. The D-R equilibrium model mean free energy of sorption and the Arrhenius equation's activation energy both confirmed that the adsorption process was physisorption. Effect of the contact time showed a sharp elevation in MB adsorption in the first 15 minutes. The adsorption kinetic process followed the pseudo-second order ($R^2 = 0.999$). Temperature elevation culminated in a reduction in adsorption capacity, suggesting an exothermic adsorption process. Thermodynamic investigation showed that the sorption process was achievable and spontaneous. There was increased randomness experienced during the interaction between the MB and the MVSF. Modified variegated sky flower stem powder can be utilized as an efficient and inexpensive adsorbent for removing methylene blue dye from aqueous solution.

Keywords: Methylene blue; adsorption; variegated sky flower; kinetic; thermodynamics

1. Introduction

Anthropogenic sources of environmental pollution have increased over the years due to effluents from different industries discharged into the environment. These effluents find their way into water bodies thereby polluting it, leading to deleterious effects on both aquatic flora and fauna. It also has harmful effects on man. Globally, A little above one hundred thousand varieties of dyes are

utilized in concerned industries and approximately 7×10^5 tons of dyes are manufactured every year [1, 2]. Dyes from industrial effluents have been implicated in environmental water pollution. Some of these industries include pharmaceutical, paper, textile, printing, leather, food, and plastic industries.

Due to their complex (aromatic) molecular structures, wastewater-containing dyes are frequently resistant to heat, oxidizing chemicals, and microbial attack and do not

readily degrade in the environment [3]. Researchers are therefore extremely concerned about the release of dyes into the environment, even at very low concentrations (< 1 ppm), for toxicological and esthetic reasons [1].

The dyes discharged into the water bodies pave way for some detrimental conditions that affect man, animals and plants such as carcinogenesis, mutagenesis, teratogenicity, chromosomal fractures, respiratory toxicity [4], skin irritation, allergic dermatitis, turbidity, an increase in the hardness of manure, the death and destruction of aquatic organisms, disruption in the photosynthesis activity of aquatic plants, and eutrophication problem. Methylene blue dye is extremely toxic when administered intravenously, emits hazardous gases such as nitrogen dioxide upon combustion, and can cause nausea and eye discomfort if it gets into direct contact with the body [5, 6]. The chemical structure of methylene blue is presented in Figure 1. Due to the extra stability that these toxic dyes acquire during the synthetic process, it is difficult to remove them from fabrics over time and under varying conditions [6]. This makes it a huge challenge to prepare effective removal strategies.

A number of conventional dye removal techniques that have been studied include ion exchange, biological degradation, irradiation, precipitation, photocatalysis, membrane filtration, ozonation, chemical oxidation, coagulation, flocculation, and solvent extraction [7]. These methods have some drawbacks, including high operational and investment expenses, insufficient dye removal, and the need to treat the residual sludge that emanates from the process. Adsorption is one of the widely accepted treatment methods due to its ease of use, low cost, and effectiveness in treating residual dye sludge. Adsorption is the least expensive and most straightforward technique

compared to all other aforementioned ones [8]. The process of adsorption can sometimes be reversible when weak van der Waals bonds exist between the adsorbent and adsorbate [8]. The adsorption of dyes has been carried out using a variety of materials. The adsorption capacity is determined by the adsorption isotherm, which characterizes the interaction between the adsorbent and adsorbate [9]. Some of the adsorbents that have been used to study the adsorption phenomenon include coffee husk [9], pumice stone [10], breadfruit leaves [11], raw *Globimetula oreophila* [12], wood waste [13], Almond shell, [14], avocado shell [15], coconut shells, golden pods, orange peels [16], *Psyllium* seeds [17], *Tectona grandis* [18], bean husk [19] and *Anisomeles malabarica* silver nanoparticles [20].

Agricultural-based materials have been used as adsorbents because of their easy availability, zero cost and reusable ability. Variegated sky flower (*Duranta erecta*) is a form of sky flower with variegated leaves. They belong to the species of flowering shrubs and the family Verbenaceae. They do not bloom so profusely and are usually grown primarily for their foliage. They are produced for their ornamental fruits and summer flower. It is a fast-growing plant that is spread by birds from domestic areas to natural reserves. They are planted around houses to beautify the environment. When trimmed, part of the multiple stems are cut off, and when left undisposed, give off putrefying smells to the environment. In order to convert waste to wealth, we used these waste stems as an adsorbent at no cost. To the best of our knowledge variegated sky flower has not been employed as an adsorbent to remove methylene dye. This work, therefore, explored the use of citric acid-modified Variegated sky flower as an adsorbent to get rid of methylene blue dye from aqueous solution.

2. Materials and methods

2.1 Chemicals

Methylene blue was obtained from Park Scientific Ltd (Northampton, UK), citric acid from Guangdong Guaghua Sci. Tech Co Ltd, China, hydrochloric acid (35.4 %) from BDH, sodium hydroxide (99.0 %) from Merck, Germany, sodium chloride (99.5 – 100 %) from Merck, Germany. The chemicals were of analytical quality, they did not need to be purified any further.

2.2 Collection and Preparation of the Adsorbent

Variiegated sky flower stem was collected from within Bowen University campus, washed using tap water, distilled water and dried in an oven at 105°C.

The variegated skyflower stem was pounded with a clean mortar and pestle and ground with an electric blender. The obtained adsorbent was sieved with a 500-micron sieve to obtain fine particles. Forty grammes (40 g) of the adsorbent was transferred into a crucible and pyrolyzed in a muffle furnace for 1 hour at 400 °C in an anaerobic condition. The activated carbon obtained from the variegated sky flower was then

allowed to cool and kept in a clean, airtight container for modification purpose.

2.3 Adsorbent modification procedure

Citric acid used for the adsorbent modification was prepared by dissolving 192.124 g of citric acid with distilled water in a 1 L flask and made up to the mark with distilled water. The adsorbent was transferred into a 250 ml beaker and 111.4 ml of 1.0 M citric acid was transferred into it and agitated using an electric orbital shaker for 1 hour 30 minutes. It was then rinsed with distilled water to remove excess citric acid by gently swirling and decanting the supernatant. The residue was oven dried at 125 °C and stored for further use and was named modified variegated sky flower activated carbon MVSF.

2.4 Preparation of the Adsorbate

This was prepared by weighing 0.25 g of methylene blue (MB) and transferred into a 250 ml standard flask, dissolved with distilled water and made up to mark. To get the appropriate concentrations for working solutions, the stock solution was serially diluted. The structure of Methylene blue is presented in Figure 1.

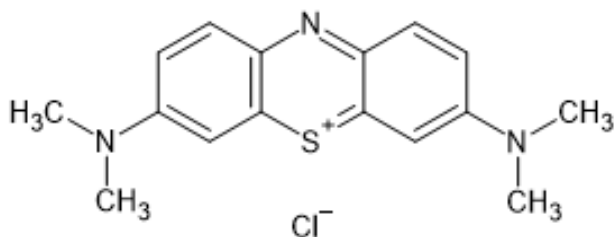


Figure 1: The structure of Methylene blue

2.5 Adsorption Experiments

The pH was studied by transferring 10 ml of 50 mg/L methylene blue solution into different beakers labelled pH 2-12. The MB was conditioned to the designated pHs by using a pH meter (JENWAY- LTD Instrument, digital model 3310) and adjusted with 0.1 M HCl and 0.1 M NaOH.

Then, 0.1 g of MVSF was transferred to each of the beakers and shaken in an electric shaker for 2 hours. They were then centrifuged after which the supernatants were taken for analysis using UV-Visible spectrophotometer at 665 nm. The initial MB concentration was studied by transferring varying concentrations of MB (50 - 400 mg/L) into beakers containing 0.1 g of MVSF and agitated at 30°C for 2 hours in a digital shaking water bath. The contact time was investigated as follows: preparation of a 100 mL, 50 mg/L MB dye concentration was progressively done in a 500-mL flasks. To each flask was added 0.50 g of MVSF. Glass stoppers were used to cover the flask before placing them on an electric stirrer at 303 K and rotated at 300 rpm until equilibrium was achieved.

In each of the experiments, Shimadzu 1800 double beam UV-VIS spectrophotometer was employed to analyze the samples. The percentage removal of MB utilizing the activated carbon obtained from the VSF is explained by equation 1:

$$q_e = \frac{(C_o - C_e)}{w} V \quad 1$$

$$\% \text{ adsorption capacity} = \frac{(C_o - C_e)}{C_o} \times 100 \quad 2$$

Where V is the volume of solution (L), q_e is the uptake capacity of the sorbent (mg/g), C_o and C_e are, respectively, the initial and final amounts of dye (mg/L), and w is the mass of the adsorbent (g).

2.6 MGO Characterization

2.6.1 Scanning electron microscopy (SEM).

A scanning electron microscope (SEM; PHENOM PRO X, MVE0224651193 Model No. 800-07334) was used to scrutinize the samples' surface morphology. SEM is a brand of electronic microscope that uses concentrated low-energy electron rays to produce enlarged sample images [19]. Different signals are produced as a result of interactions between an electron's shaft and the sample's atomic components. The signals produced by the SEM are used to infer details about the surface characteristics, composition, and environment of the sample.

2.6.2 FTIR

Agilent Technologies Cary 630 Fourier transform infrared (FTIR) spectrometer was employed to record MVSF spectra. The spectra measurements were done between 4000 and 600 cm^{-1} . The FTIR spectra revealed the functional group (s) on the MVSF without and with MB adsorption.

3. Results and discussion

3.1 Characterization of the adsorbent

3.1.1 Scanning Electron Microscopy (SEM)

Analysis

The surface morphology and pore dispersion of MVSF are revealed using scanning electron microscopy. Images of MVSF was exhibited in Figures 2a (without MB) and 2b (with MB). Before the adsorption of MB more available pores were present on the surface structure. These characteristics of MVSF would be conducive for the capture of the target dyes. After the adsorption of MB, the pores became filled. The number of available pores reduced drastically.

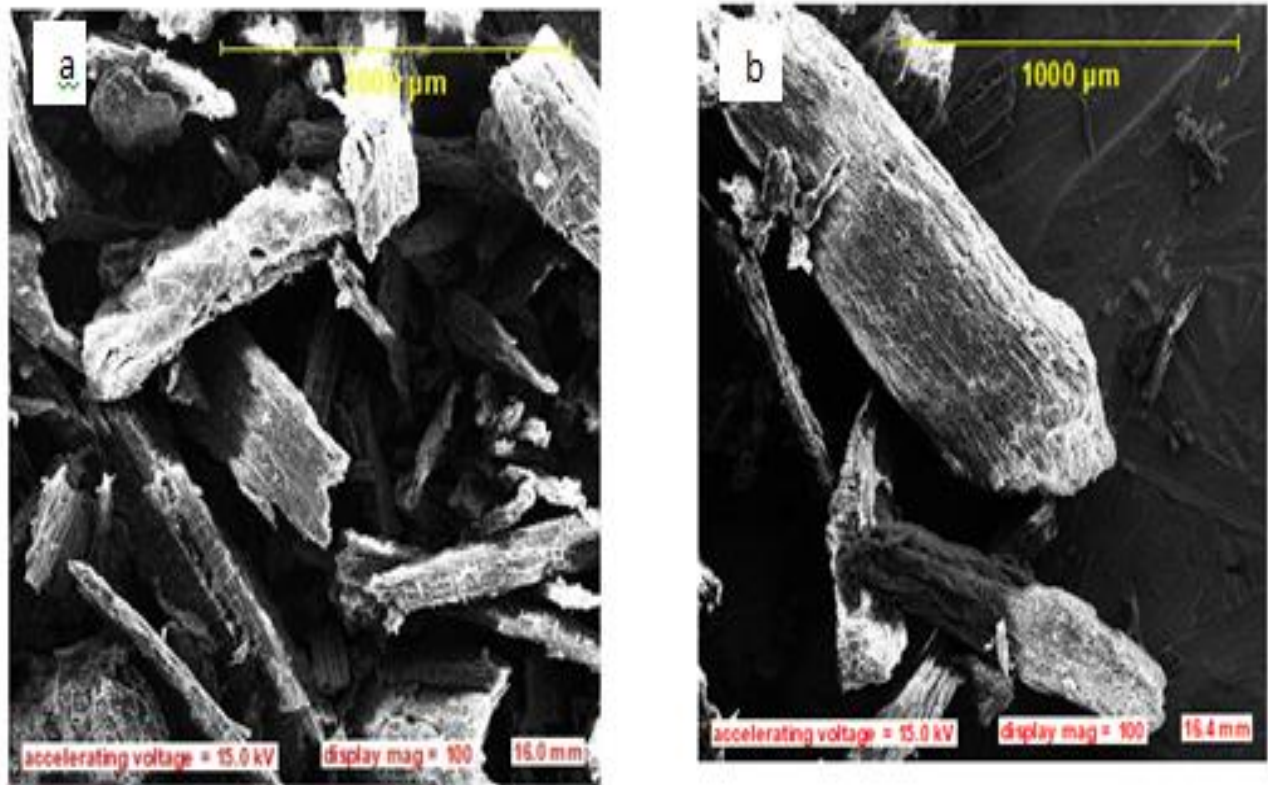


Figure 2: The Scanning electron microscopy of modified Variegated Sky flower (a) without MB and (b) with MB

3.1.2 FTIR Spectra Analysis

The FTIR spectrum of the modified variegated sky flower without methylene blue is presented in Figure 3a, while that of the modified variegated sky flower with methylene blue is presented as 3b. The analysis of Figure 3a revealed characteristics peaks at 3190 cm^{-1} , 1681 cm^{-1} , and 1182 cm^{-1} which correspond to O-H stretch, C=O stretch and C-O stretching vibration respectively for modified variegated sky flower. The peaks were shifted to lower frequencies of 3185 cm^{-1} and 1702 cm^{-1} respectively for the O-H vibrational band and

the C=O vibrational band after the modification of the variegated sky flower with methylene blue as shown in Figure 3b. This signifies the chemical interactions of the OH and C=O functional group molecules with other molecules around during the process of adsorption of methylene blue. The C-O band appeared almost unchanged at frequency of 1183 cm^{-1} in the spectrum of the modified variegated sky flower with methylene blue (Figure 3b). This signifies that no chemical interactions occurred between the C-O functional group and any other molecule present around it during the adsorption process [21, 22].

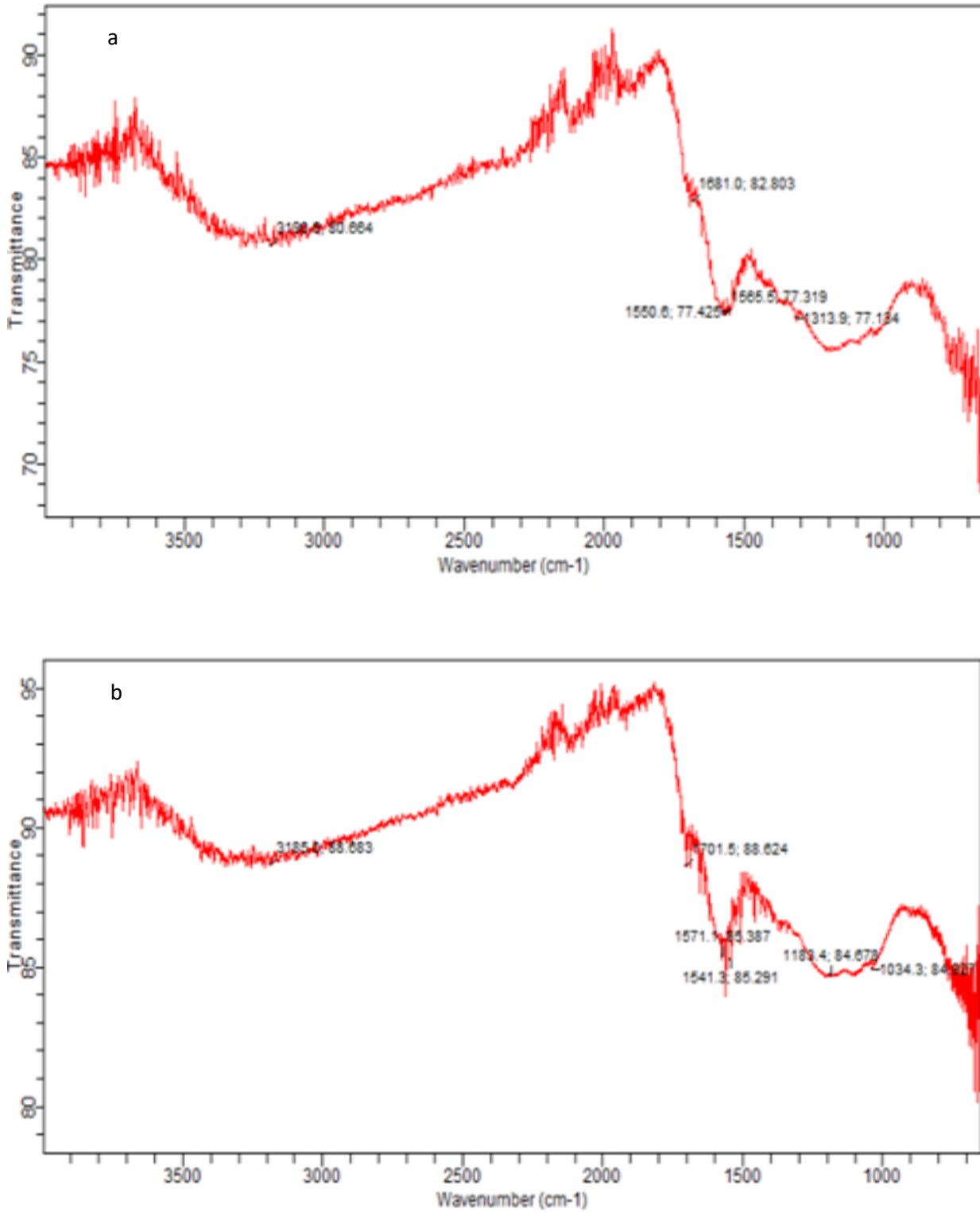


Figure 3 The Fourier Transform infrared spectroscopy (FTIR) of modified Variegated Sky flower (a) without MB and (b) with MB

3.2 The effect of point of zero charge and pH

The impact of pH is an important factor in the determination of the sorption capacity of dyes since pH influences the facile charge of the adsorbent and also affects the chemical structure of the sorbate [8]. Figure 4a shows that MB dye adsorption by MVSF was pH dependent. Experimental observation revealed that the sorption uptake of MB rose sharply from pH 2 – 5. The maximum sorption capacity (108.7 mg/g) was achieved at pH 5. At the acidic region (low pH), there was competition for the adsorption site by both the adsorbate and hydrogen ions. The protonation of the adsorption site and the consequent electrostatic repulsion are responsible for the low adsorption capacity at

the high acidic region. As the pH increases, the adsorption capacity increases because more spaces are available for the interaction of the adsorbate with the adsorbent.

The pH point of zero charge (pHPZC) of MVSF is shown in Figure 4b. The value was ascertained where the curve cuts through the Δ pH axis (Figure 4b). The pHPZC observed was at 5.0 for MVSF. Thus the maximum pH and the pHPZC value are coincidentally same. When there is elevation of the pH value beyond that of the pHPZC, adsorption of cations is favoured, while anions adsorption is enhanced when the pH value is reduced when compared with pHPZC. Since the pHPZC of MVSF was obtained at 5.0, this implied that the best pH value for optimum adsorption of MB is 5.0.

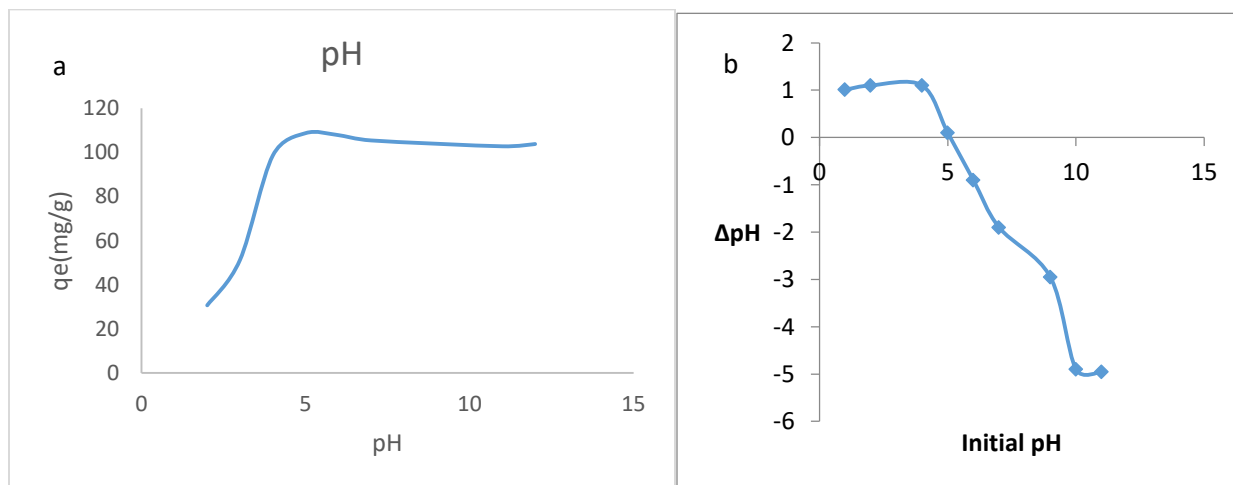


Figure 4: Graph of a. pH and b. point of zero charge of the sorption of Methylene blue on modified Variegated Sky Flower

3.3 Influence of initial concentration of MB

The initial dye concentration sheds light on the sorbent's properties and the type of interactions with the adsorbate. The dye adsorption onto MVSF was explored from 250 – 400 mg/L initial dye concentration as presented in Figure 5. The adsorption capacities of the MVSF increased from 44.1 to 93.4 % as the initial methylene blue concentration rose from 250 mg/L to 300

mg/L. The adsorption attained equilibrium beyond 300 mg/L methylene blue initial concentration. The concentration gradient and the accessibility of active sites may be the driving forces behind the elevation of the adsorption capacity at low dye concentrations. These active sites became saturated at higher dye concentrations such that the adsorption capacity remains the same [23].

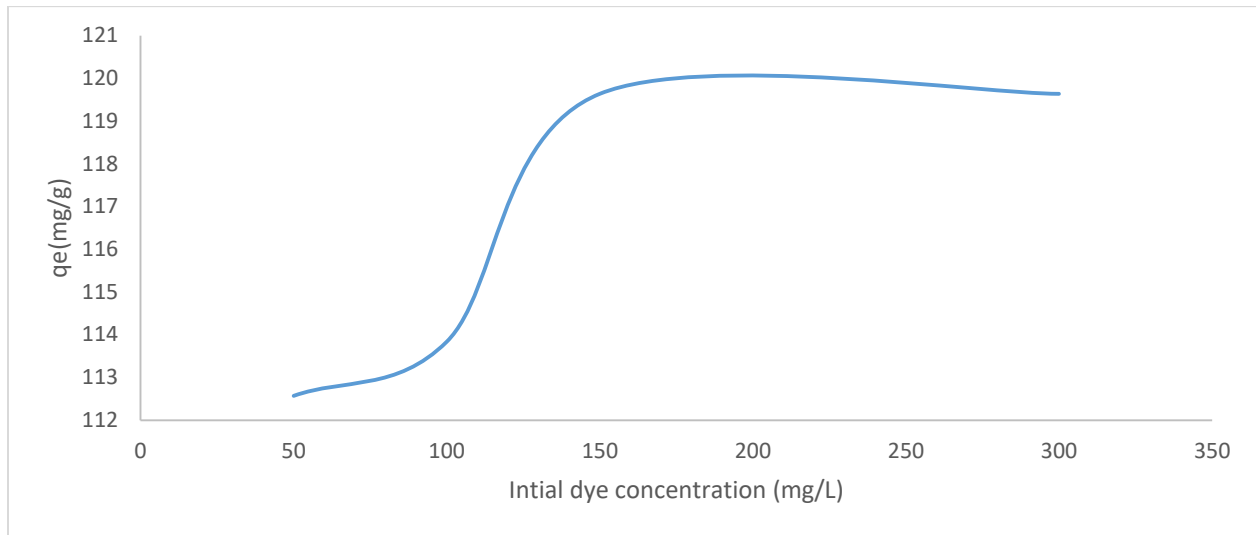


Figure 5: Influence of initial dye concentration on the sorption of Methylene blue on modified Variegated Sky Flower

3.4 Influence of contact time

Contact time refers to the interaction between the sorbate molecules and the sorbent. As the contact time increases the probability of the adsorbate molecule interacting with the active site of the adsorbent also increases. From Figure 6, the adsorption capacity of MVSF for MB rose sharply from time 0 to 15

minutes after removing 30 mg/g of MB. This was the result of the availability of large population of accessible sorption sites. The adsorption removal rate increased gradually from 15 – 70 minutes with 45 mg/g of MB removed after 70 minutes. This is ascribed to a reduction in the population of active sites. The adsorption reached equilibrium after 70 minutes.

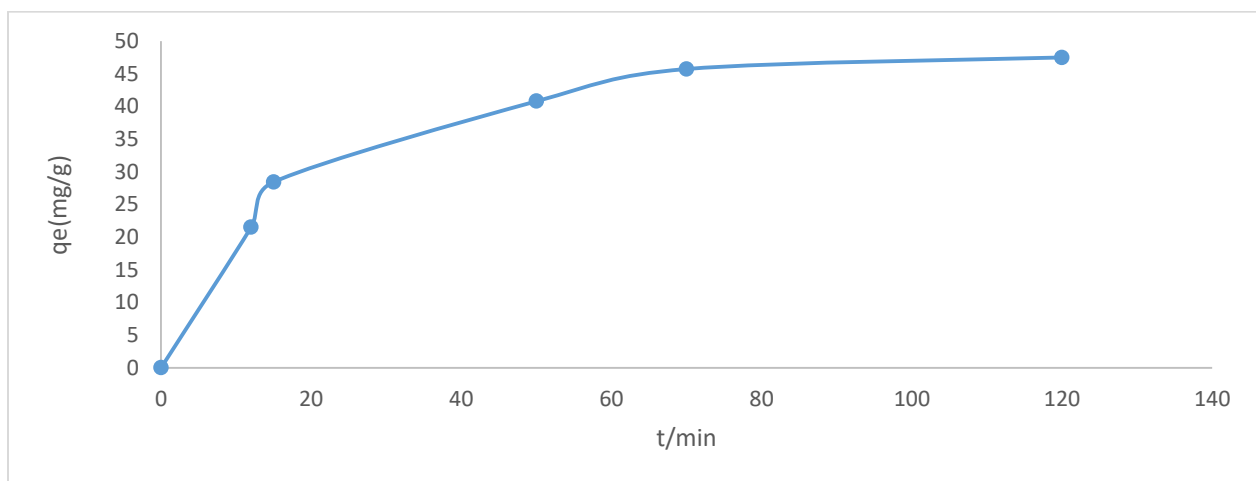


Figure 6: Influence of contact time on the adsorption of Methylene blue on modified Variegated Sky Flower

3.5 Influence of temperature

Temperature influences the adsorption process as it appreciably affected the uptake capacity as well as the surface characteristics of the sorbent. It also explains how mobile and soluble the dye molecules would be in an aqueous solution [9]. Additionally, as the temperature rises, the rate of adsorbate molecule diffusion through the external boundary layer of the sorbent and within their inner pores increases, and the viscosity of the solution decreases. As shown in Figure 7, experiments were conducted to determine the impact of temperature on the sorption of methylene blue dye by MVSF while maintaining a consistent MB dye

concentration to sorbent dose (10 mL of 50 mg/L and 0.5 g of MVSF). The result demonstrated that the methylene blue dye adsorption onto MVSF involved evolution of heat, where an elevation of temperature led to a decrease in adsorption capacity [9]. In contrast to 6.19 mg/g at 318 K, 21.2 mg/g of dye was adsorbed at 303 K. This finding might be the result of weaker binding interactions that aid in the separation of molecules of dye from the sorbent surface, resulting in lower sorption as the temperature increases. This finding is in line with those made when MB was adsorbed onto cashew nut-activated carbon [24] where it was discovered that the sorption process involved the evolution of heat.

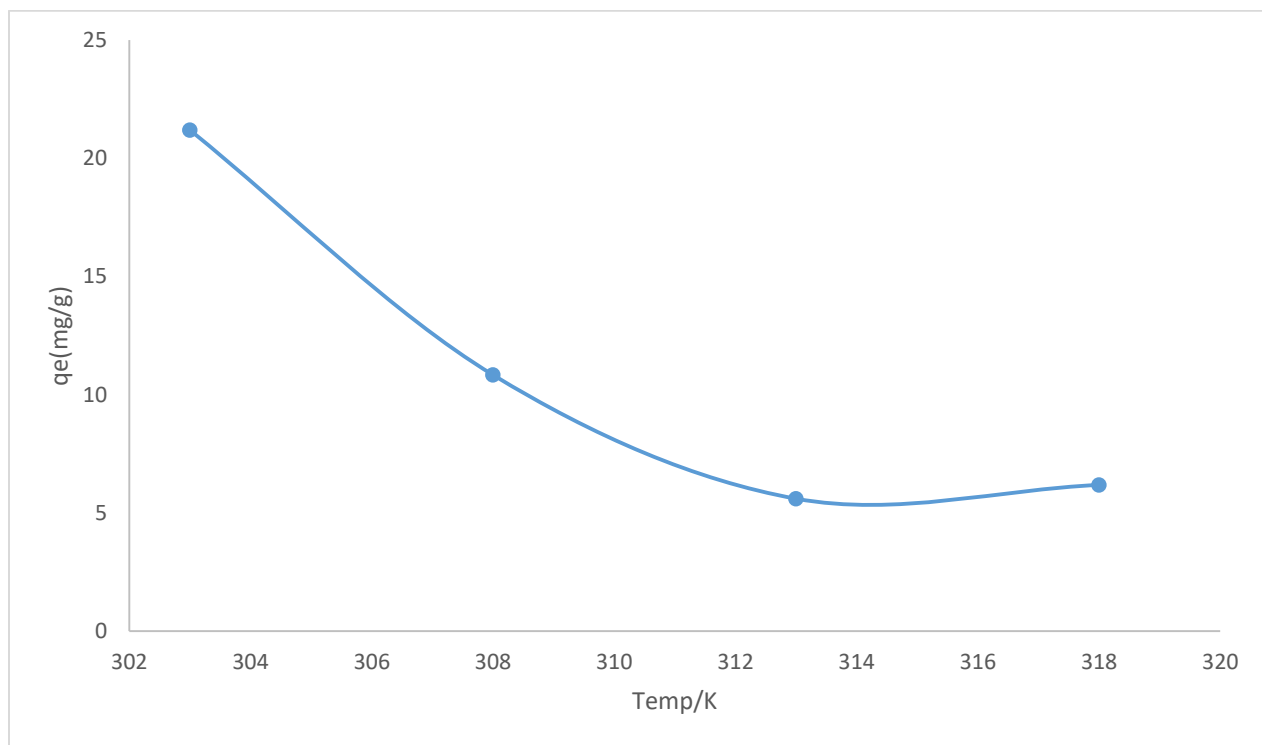


Figure 7: The influence of temperature on Methylene blue adsorption on modified variegated sky flower.

3.6 Effect of kinetic studies

A kinetic investigation can be carried out for batch adsorption procedures in order to control the rate of the reaction and provide the optimal conditions for the parameters required for the study. Three kinetic models namely pseudo-first order, pseudo-second order [25] and Elovich models were employed to analyze the experimental adsorption kinetic data. In adsorption processes, these three models are widely used to explore the variables that affect the process, such as the sorption surface, chemical reactions, and/or diffusion mechanisms [9, 26].

3.6.1 Pseudo- first order kinetics

The below equation 3 was used to illustrate the integral form of the pseudo-first order kinetic models.

$$\log(q_e - q_t) = \log q_e - \frac{c_1}{2.303}t \quad 3$$

where q_t is the quantity of dye uptake per unit mass of sorbent over time (mg g^{-1}), q_e is the amount of dye uptake at equilibrium (mg g^{-1}), and c_1 is the rate constant of pseudo-first-order adsorption (min^{-1}). A graph of $\log(q_e - q_t)$ versus t results in a straight line with $\log q_e$ as the intercept and k_1 the slope. Figure 8a presents the pseudo-first order plot. A pseudo- first order kinetic plot of $\log(q_e - q_t)$ against time (t) produced straight lines having lower correlation values ($R^2 = 0.877$) as reported in Table 1. The first-order mechanism is not suitable for explaining the kinetic process because the values of q_e obtained from the graph indicated a significant discrepancy from the experimental data.

3.6.2 The pseudo-second order kinetic

The kinetic model, a pseudo-second order (equation 4) is given as

$$\frac{t}{q_t} = \frac{1}{c_2 q_e^2} + \frac{1}{q_e} t \quad 4$$

Where t is the experimental time (in mins), c_1 and c_2 are the rate constants for the pseudo-first and second order respectively, q_e and q_t are the respective equilibrium sorption amount, and the quantity of dye adsorbed at time t . The plot of $\frac{t}{q_t}$ and t results in a straight line in which $\frac{1}{q_e}$ is the slope and $\frac{1}{c_2 q_e^2}$ is the intercept as depicted in Figure 8b. The pseudo-second order model used to analyze the experimental results and determine the kinetics of adsorption of MB dye on MVSF, gave better fit ($R^2 = 0.999$) due to the close proximity of the calculated adsorption capacity to the experimental value as well as the low value of the sum of square error Δq . Similar adsorption kinetics were obtained for functionalized bean husk [19], *Tectona grandis* [18] and *Senna fistula* [2]. The result implies that a physical process involving van der waal forces of interaction between the dye and the adsorbent controlled the overall rate of the adsorption process.

3.6.3 Elovich kinetic model

Elovich kinetic model is employed to explain the adsorption kinetics on heterogeneous solid. The equation is expressed as

$$q_t = \left(\frac{1}{\delta}\right) \ln \gamma \delta + \left(\frac{1}{\delta}\right) \ln t \quad 5$$

Where γ and δ represent, respectively, the initial rate of sorption [mg. (g min)^{-1}] and the level of the surface coverage as well as the energy of activation for chemisorption (g.mg^{-1}). The $\frac{1}{\delta}$ value expresses the number of accessible sites for adsorption, $(\ln \gamma \delta)$ expresses the amount of adsorption when $(\ln t)$ is equivalent to zero. The internal diffusion

is the adsorption process' slowest stage if the graphs are linear and go through the origin. Elovich isotherm model is not appropriate for

elucidating the equilibrium sorption process since its correlation factor is far from unity ($R^2 = 0.897$) as revealed in Figure 8c.

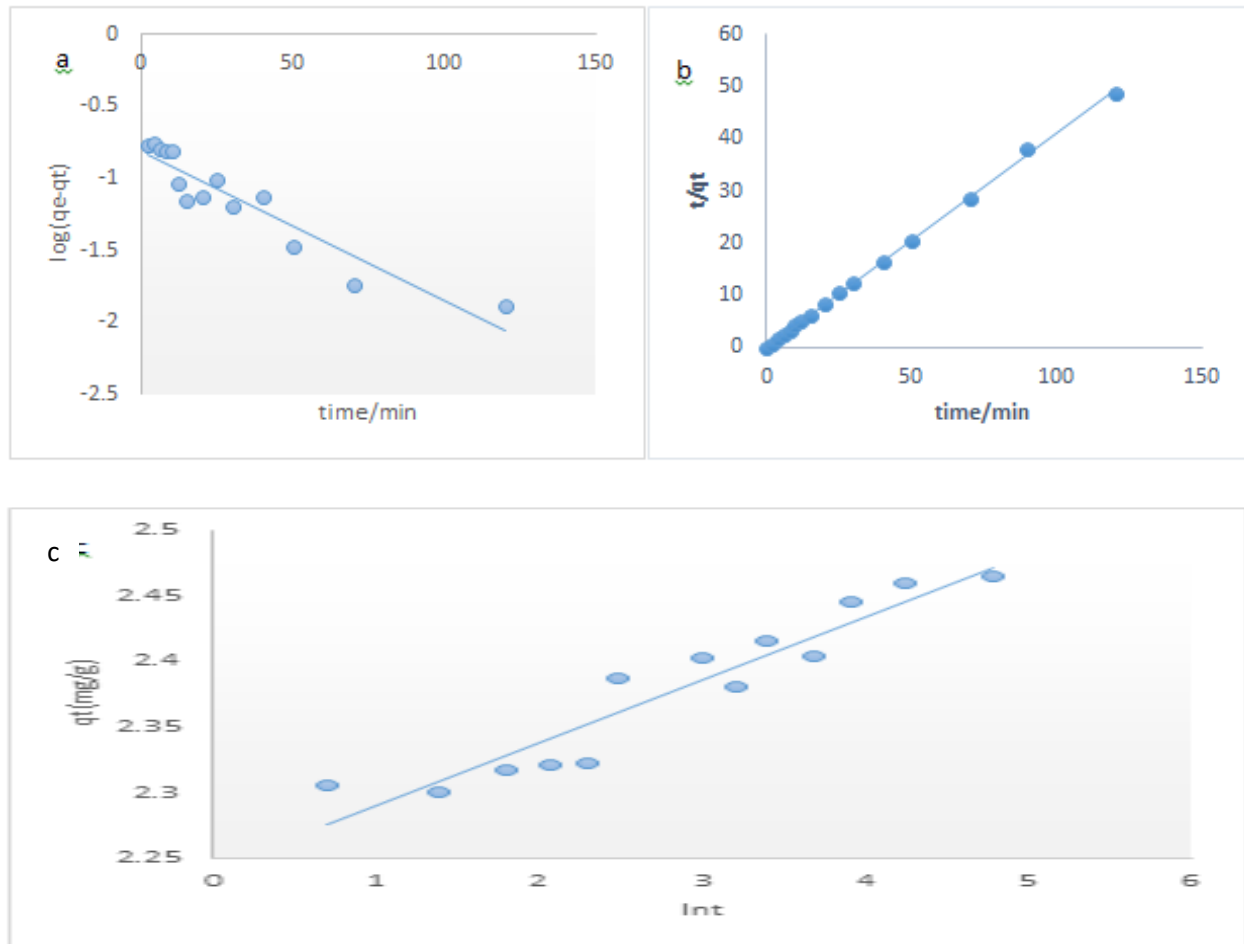


Figure 8a: Pseudo - first order b. Pseudo -second order c. Elovich kinetic plots for the sorption of Methylene blue on modified Variegated sky flower

Table 1: Kinetic models for the sorption of Methylene Blue on modified Variegated Sky Flower

Pseudo- first order	Pseudo - second order	Elovich
$q_{e(exp)} (mgg^{-1}) = 2.439$	$q_{e(exp)} (mgg^{-1}) = 2.439$	$\delta = 21.0$
$q_{e(calc)} (mgg^{-1}) = 2.26$	$q_{e(calc)} = 2.439$	$\gamma = 1.39 \times 10^{19}$
$c_1 (min^{-1}) = 0.0104$	$c_2 (gmg^{-1}min) = 1.30$	$R^2 = 0.897$
$\Delta q = 0.127$	$\Delta q = 2.66 \times 10^{-4}$	
$R^2 = 0.877$	$R^2 = 0.999$	

3.7 Adsorption models

Adsorption models are often employed in the study of the equilibrium parameters and the adsorption characteristics. Additionally, it helps to comprehend the type of interactions occurring between the sorbate and the sorbent. They also offer some details on the most desirable and possible uses of the adsorbent. In this experimental investigation, the sorption of Methylene blue dye, selected as the sorbate on the surface of the sorbent prepared from the variegated sky flower was evaluated for four distinct adsorption isotherm models, the Langmuir, Freundlich, Temkin, and Dubinin-Radushkevich (D-R).

3.7.1 Langmuir model

The Langmuir isotherm model gives details about the active sites present on the adsorbent surface as well as the sites saturation, provided all the accessible sites are involved and maximum sorption is achieved [27]. Equation 7 serves as a linear representation of the Langmuir model:

$$\frac{C_e}{q_e} = \frac{1}{K_L Q_{max}} + \frac{C_e}{Q_{max}} \quad 6$$

where Q_{max} is the adsorbent's maximum uptake capacity (mgg^{-1}), K_L is the Langmuir constant associated with the sorption energy, q_e is the MVSF's sorption capacity, while C_e is the concentration at equilibrium of MB dye.

The separation factor, abbreviated R_H , which represents the favorability of adsorption, is another crucial piece of knowledge that can be gleaned from the Langmuir isotherm. The equation below can be used to calculate the R_H values:

$$R_H = \frac{1}{K_L C_o + 1} \quad 7$$

C_o represents the initial amount of the MB dye solution. R_H values determine the type of sorption, such as irreversible if R_H values are equal to 0. In addition, R_H values greater than

1 are unfavorable, while R_H values between 0 and 1 are favorable. Langmuir isotherm revealed from Table 2 that the dimensionless quantity R_H value less than 1 represents the favourability of the sorption process. The maximum sorption capacity was 107.5 mg/g.

3.7.2 Freundlich isotherm

The Freundlich model is founded on the sorption of heterogeneous surface sites of varying affinities. The assumption of this model is that there is an initial occupation of the stronger binding sites such that subsequent binding strength reduces with the increasing level of occupation of the site. The Freundlich straight-line equation is given by

$$\ln q_e = \ln K_F + \frac{1}{n} \ln C_e \quad 8$$

Where q_e is amount of sorbate sorbed per unit mass of sorbent (mgg^{-1}); K_F ($\text{mgg}^{-1} \cdot \text{Lmg}^{1/n}$) and n are Freundlich constants which indicate the uptake capacity of the sorbent that is affiliated, respectively, with the bonding energy and the strength of adsorption; C_e is the amount of the adsorbate at equilibrium (mgL^{-1}). The plot of $\ln q_e$ against $\ln C_e$, if linear, implied that the Freundlich model correlates with the data. Other constants that can be determined from the straight line plot are the intercept ($\log K_F$) and the slope (n^{-1}). The value of n is greater than 0 ($n = 2.91$) which is a measure of the sorption strength and becomes more heterogeneous as its value increases above 0. The correlation factor obtained was 0.996.

3.7.3 Temkin model

The Temkin isotherm model surmises that all molecules have heat of sorption that reduces linearly as the coverage of the sorbent surface increases. The straight line equation of Temkin model is written as:

$$q_e = D \ln A + D \ln C_e \quad 9$$

and $D = \frac{RT}{e}$ 10

T(K) is the temperature, and R is the gas constant ($Jmol^{-1}K^{-1}$). The heat of sorption is represented by the constant e ($Jmol^{-1}$), while the highest binding energy is represented by the constant A ($Lmol^{-1}$). The graph of q_e versus lnC_e will yield D and enable the determination of the constant A.

3.7.4 Dubinin–Radushkevich (D–R) isotherm

The D–R model is employed to differentiate between chemical and physical adsorption and to determine the distinct free energy of adsorption. It is also used to determine porosity, free energy and characteristics of the sorbent. It elucidates how subcritical vapours adsorb to microscopic solids to ensure procedural pore packing. Additionally, it guarantees the typical adsorbent porosity, particularly for carbonaceous materials.

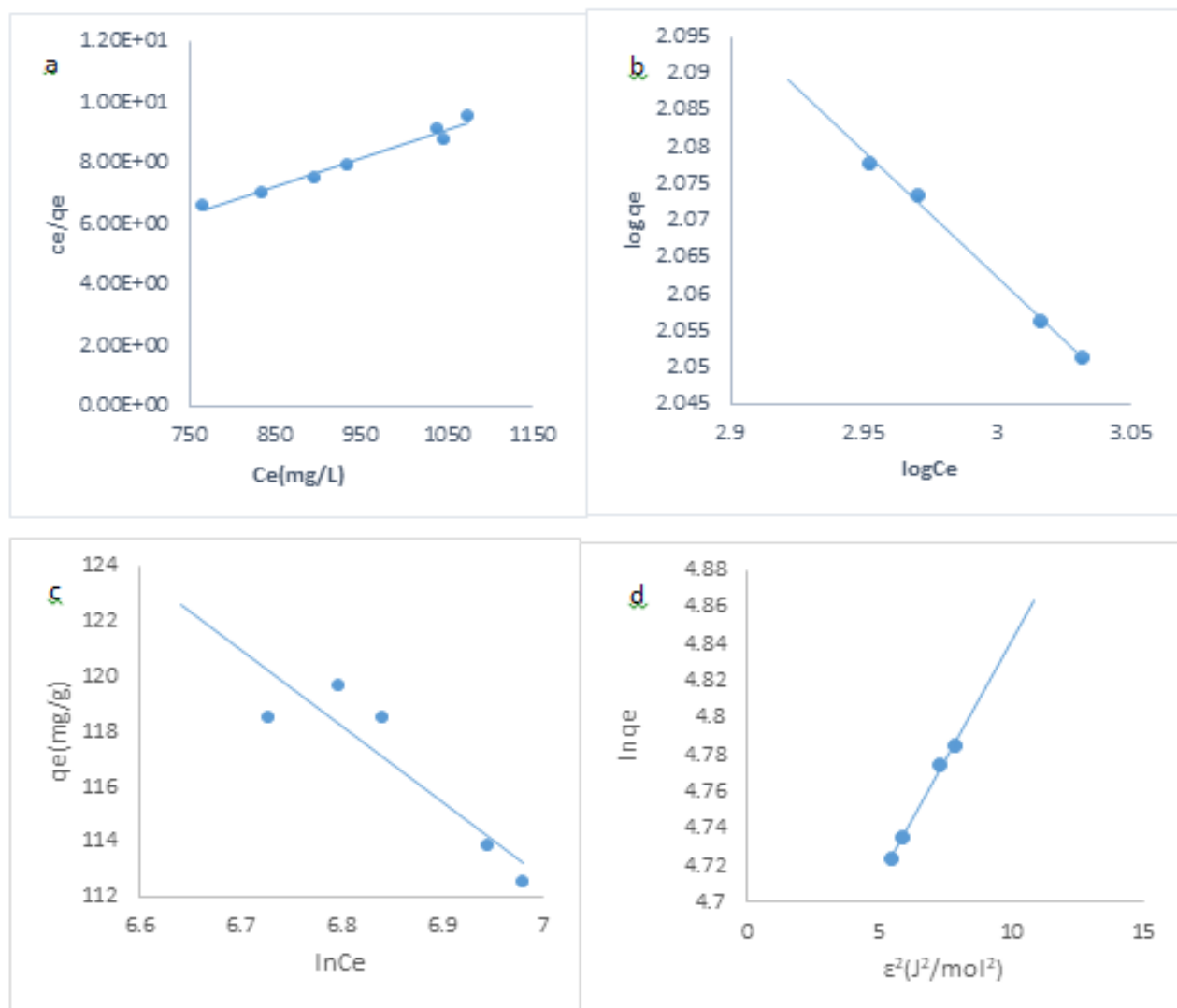


Figure 9: Graph of a. Langmuir b. Freundlich c. Temkin and d. Dubinin–Radushkevich (D–R) models for the sorption of Methylene Blue on Variegated sky Flower

Table 2: Equilibrium models for the sorption of Methylene Blue unto modified *Variegated Sky Flower*

Langmuir	Freundlich	Temkin	D-R
$X_o = 107.5 \text{ mg/g}$	$K_F = 1242.8$	$e = 91.2$	$q_e = 97.7 \text{ mg/g}$
$c = 0.0125$	$n = 2.91$	$A = 64761$	$\gamma = 0.0259$
$R_H = 0.08$	$R^2 = 0.996$	$R^2 = 0.826$	$E = 4.39 \text{ Jmol}^{-1}$
$R^2 = 0.9699$			$R^2 = 0.992$

The equation is expressed as:

$$\ln q_e = \ln q - \gamma \left[RT \ln \left(1 + \frac{1}{c_e} \right) \right]^2 \quad 11$$

Where γ represents a constant denoting the adsorption energy, q_e represents the concentration of the adsorbate adsorbed at equilibrium, p gives the highest sorption capacity, ε is the Polanyi potential, and is represented by

$$\varepsilon = RT \ln \left(1 + \frac{1}{c_e} \right) \quad 12$$

The linear expression for equation 12 is,

$$\ln q_e = \ln p - \gamma \varepsilon^2 \quad 13$$

The γ and p values can be obtained from the intercept and gradient of the graph of $\ln q_e$ against ε^2 respectively.

The average free energy of sorption, E , can be determined from the equation

$$E = \frac{1}{\sqrt{2\gamma}} \quad 14$$

The value of E obtained for the adsorption of MB was 4.39 J/mol. This implies that the uptake of MB by MVSF is physisorption in nature.

Comparing the four sorption isotherms—Langmuir, Freundlich, Temkin, and Dubinin-Radushkevich (D-R) displayed in Figures 9a,b,c and d, the Freundlich and Dubinin-Radushkevich isotherms, which had the highest R^2 values at 0.996 and 0.992, respectively, best fit the adsorption data. This may be credited to the high degree of surface coarseness and the presence of additional oxidation groups, which facilitate the multilayer sorption of MB onto the MVSF [28]. Additionally, interactions of $\pi - \pi$ electrons between MB and MVSF as well as the effect of the simple electrostatic interactions result in higher uptake capacity [28, 29, 30, 31].

Table 3 presents the comparison between various adsorbent uptake capacities and that of MVSF. It is evident from Table 3 that when compared to other adsorbents, the modified variegated sky flower has the highest sorption capacity.

Table 3: Uptake capacities for different adsorbents for methylene blue

Adsorbent	Uptake capacity (mgg ⁻¹)	Reference
modified <i>Strychnos potatorum</i> seeds (SMSP)	78.8	[30]
photocatalytic CuBTC/ZnO chitosan composites	50.1	[32]
<i>Anisomeles malabactica</i> silver nanoparticles	97.1	[20]
Cellulose Acetate Nanofibrous Membranes Modified by Polydopamine	88.2	[33]
Modified sawdust	5.464	[34]
<i>Solanum macrocarpon</i>	53.4	[35]
Modified Pumice Stone	15.87	[15]
Natural Saudi red clay	50.25	[23]
Modified Variegated Sky Flower	107.5	This study

3.8 Thermodynamics

The study of the viability, spontaneity, and enthalpy change of sorption onto the sorbent surface, and the mechanism of sorption depends heavily on the determination of thermodynamics research.

The determination of thermodynamics studies is very vital in the study of how feasible and spontaneous the adsorption mechanism is as well as the enthalpy change of sorption onto the sorbent surface. The

thermodynamic parameters to be evaluated include the entropy change ΔS° , the enthalpy change ΔH° and the free energy change ΔG° . The equations are the following:

$$\Delta G^{\circ} = \Delta H^{\circ} - T\Delta S^{\circ} \quad 15$$

$$\ln K = \frac{\Delta S}{R} - \frac{\Delta H}{RT} \quad 16$$

Where the distribution coefficient, thermodynamic temperature in Kelvin, and the gas constant are denoted respectively by K, T and R.

Table 4: Thermodynamic quantities for the sorption of SO on modified *Variegated Sky Flower*

Adsorbent	ΔH (kJ/mol)	ΔS (J/mol)	ΔG			E_a (kJ/mol)
			308 K	313 K	318 K	
MVSF	-9.16	21.5	-15.8	-15.9	-16.0	7.60

Figure 10 presents the plot of $\ln K$ against $1/T$. From the plot, the values of ΔH^0 , ΔS^0 and ΔG^0 were determined. The values of ΔH^0 and ΔS^0 obtained are -7.17 kJmol^{-1} and 21.5 J/mol respectively. These indicate that heat is given off (exothermic) during the process of adsorption and shows increased interaction at the sorbent – sorbate interface respectively. The ΔG^0 value obtained revealed that the sorption process is achievable and spontaneous. Similar result was obtained for *Carica papaya* [36].

The activation energy for the process of adsorption was derived from the expression below:

$$\ln k = \ln A - \frac{E_a}{RT} \tag{17}$$

where k represents the rate constant, A is the Arrhenius factor, and E_a is the energy of activation. The activation energy value (7.6 kJ/mol) obtained revealed that the sorption process is physisorption. The thermodynamic results that MVSF can be employed as a possible and effectual adsorbent for removing MB in an aqueous solution.

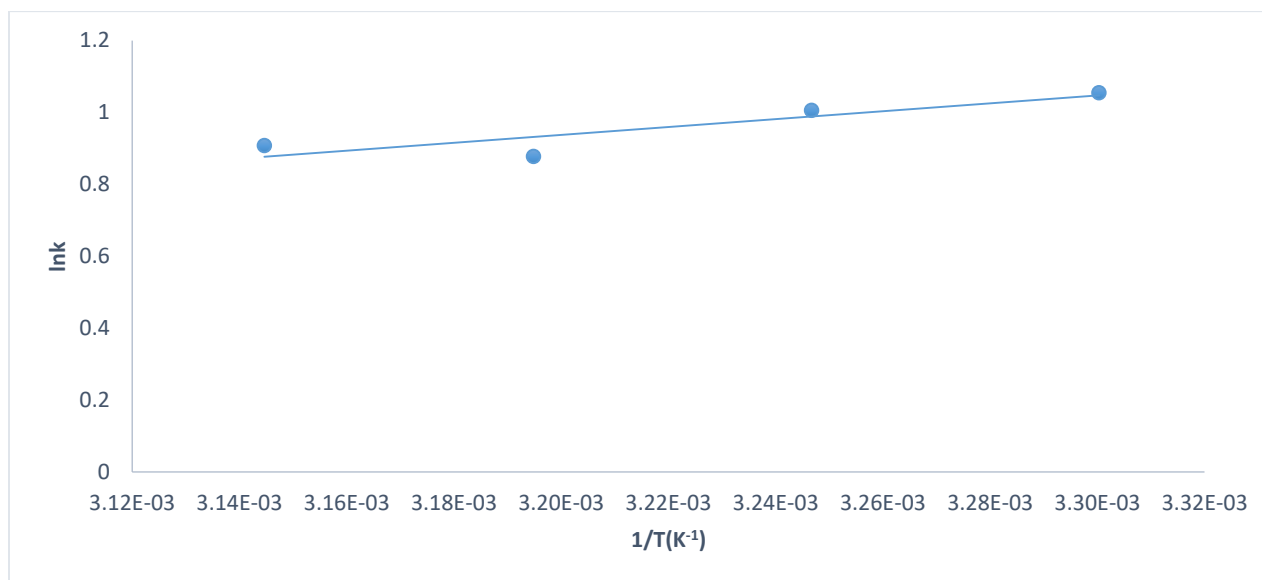


Figure 10: Thermodynamic plot of $\ln K$ vs $1/T$ for the sorption of MB by modified variegated sky flower

Conclusion

In order to eliminate MB from aqueous solutions, the effectiveness of the stem of the variegated sky flower was investigated in this study. Variegated sky flowers have been successfully used in experiments to provide inexpensive adsorbents. The optimum MB sorption occurred at a pH of 5.00. The presence of available pores on variegated skyflower as a result of activation by phosphoric acid improved the sorption of MB. Freundlich and Dubini-Raduchkevich models best fitted the adsorption equilibrium data.

The physical adsorption process was confirmed by the average free energy of sorption in the D-R equilibrium model and the activation energy in the Arrhenius equation. The kinetic adsorption process was best explained by the pseudo-second order model. The feasibility and spontaneity of the sorption activity were confirmed by ΔG° . The process of adsorption involved heat evolution, and there was increased disorderliness between the sorbate and the sorbent. This study reveals that variegated sky flower was both a cheap and effective adsorbent for removing MB from aqueous solutions.

Declaration of Competing Interest

There is no conflict of interest among the authors.

References

- [1] Mousavi, S. A. Mahmoudi, A. Amiri, Darvishi S. P., & Noori, E. (2022). Methylene blue removal using grape leaves waste: optimization and modeling. *Applied Water Science*, 12: 112
- [2] Ajaelu C. J., Oyedele, O., Ikotun A. A., & Faboro E. O. (2022). Safranin O dye removal using *Senna fistula* activated biomass: Kinetic, equilibrium and thermodynamic studies. *Journal of Nigerian Society of Physical Science*, 5. 951
- [3] Nekouei, F., Nekouei S., Tyagi, I., & Gupta V.K., (2015). Kinetic, thermodynamic and isothermal studies for acid blue 129 removal from liquids using copper oxide nanoparticle-modified activated carbon as a novel adsorbent. *Journal of Molecular Liquid*, 201 :124
- [4] Razzaq, S, Akhtar, M, Zulfiqar, S, Zafar, S, Shakir, I, Agboola, P.O, Haider, S, Warsi.M. F.& (2021). Adsorption removal of Congo red onto L-cysteine/ rGO/PANI nanocomposite: equilibrium, kinetics and thermodynamic studies. *Journal of Taibah University for Science*, 15 (1): 50–62.
- [5] Shakoor S & Nasar A. (2017). Adsorptive treatment of hazardous methylene blue dye from artificially contaminated water using *cucumis sativus* peel waste as a low-cost adsorbent *Groundwater for Sustainable Development*. 5: 152 – 159.
- [6] Dindorkara, S. S., Patel, R. V., & Yadav A (2022). Adsorptive removal of methylene blue dye from aqueous streams using photocatalytic

- CuBTC/ZnO chitosan composites
Water Science Technology, 85 (9) :
2748.
- [7] Noorimotlagh Z, Mirzaee, S.A.
Martinez, S.S. Alavi, S. Ahmadi, M.
Jaafarzadeh, N. (2019) Adsorption of
textile dye in activated carbons
prepared from DVD and CD wastes
modified with multi-wall carbon
nanotubes: equilibrium isotherms,
kinetics and thermodynamic study.
Chemical Engineering Research and
Design, 141 : 290–301,
- [8] Hussain, S M., Kamran, Khan, S. A.
Shaheen, K., Shah, Z., Suo, H.,
Khan, Q., Shah, A. B., Rehman, W.
U., Al-Ghamdi, Y. O., Ghan, U.
(2021). Adsorption, kinetics and
thermodynamics studies of methyl
orange dye sequestration through
chitosan composites films.
*International Journal Biological
Macromolecule*, 168 : 383–394.
- [9] Cheruiyot, G. K., Wanyonyi, W. C.,
Kiplimoa, J. J.. Maina, E. N. (2019).
Adsorption of toxic crystal violet dye
using coffee husks: Equilibrium,
kinetics and thermodynamics study.
Scientific Africana, 5 : 1 - 12
- [10] Derakhshan, Z.. Baghapour, M. A.,
Ranjbar, M., Faramarzian, M..
(2013). Adsorption of Methylene
Blue Dye from Aqueous Solutions by
Modified Pumice Stone: Kinetics and
Equilibrium Studies. *Health Scope*.
2(3): 136–44.
- [11] Ajaelu, C. J. Dawodu, M. O.,
Abogunrin, O., Otolorin., J. A.
(2013). Kinetics and Equilibrium
Studies of the Biosorption of Heavy
metal ions from Simulated
Wastewater using Breadfruit leaf
(*Artocarpus artilis*). *European
Journal of Scientific Research*. 98(1):
85-97.
- [12] Ajaelu, C. J., Faboro, E. O. (2021).
Adsorption of copper (II) ions onto
raw *Globimetula oreophila* (Afomo
ori koko) leaves. *African Journal of
Biotechnology*, 20(3) : 122-133.
- [13] Adesokan, S. A. & Giwa, A. A., &
Bello, I. A. (2021). Removal of
trimethoprim from water using
carbonized wood waste as adsorbents
*Journal of Nigerian Society of
Physical Sciences*. 3 344–353
- [14] Ben Arfi, R. Karoui,
S., Mougine, K., & Ghorbal,
A. (2017). Adsorptive removal of
cationic and anionic dyes from
aqueous solution by utilizing almond
shell as biosorbent. *Euro-
Mediterranean Journal of
Environmental Integration*, 2: 20
- [15] J. Georgin, B. D. Marques, J. D.
Salla, E.L. Foletto, D. Allasia, G.L. D
otto. Removal of Procion Red dye
from colored effluents using H₂SO₄-
/HNO₃-treated avocado shells (*Persea
Americana*) as adsorbent,
*Environmental Science Pollution
Resource*, 25 (2018), 6429-6442
- [16] Tran, H.N., You, S.-J. & Chao, H.-
P. (2017). Insight into adsorption
mechanism of cationic dye onto
agricultural residues-derived

- hydrochars: Negligible role of $\pi - \pi$ interaction, I, 34 (2017) 1708-1720.
- [17] M. Malakootian, M.R. Heidari. Reactive orange 16 dye adsorption from aqueous solutions by psyllium seed powder as a low - cost biosorbent: kinetic and equilibrium studies. *Applied Water Science*, 8 (2018) 212
- [18] Ajaelu, C. J., Ibronke, L. Oladinni, A. B. (2019). Copper (II) ions adsorption by Untreated and Chemically Modified *Tectona grandis* (Teak bark): Kinetics, Equilibrium and thermodynamic Studies. *African Journal of Biotechnology*, 18(14) : 296-306.
- [19] Bello O.S., Alao, O.C., Alagbada, T.C., Olatunde, A.M. (2019). Biosorption of ibuprofen using functionalized bean husks, *Sustain. Chem. Pharm.* 13 (2019) 100151
- [20] Prabhakar, M. ., Gomathi, K., Venkatesh, R., Stalany, V. M., Vijayan, D. S., Sassykova, L. R., Sendilvelan, S., Priya, V. S., Jijina, G. O., Selvaraj, R. (2022). Isothermic and Kinetic Study on Removal of Methylene Blue Dye Using Anisomeles malabarica Silver Nanoparticles: An Efficient Adsorbent to Purify Dye-Contaminated Wastewater. *Adsorption Sci. & Technology*, 2022: 1 - 7
- [21] Ikotun, A. A., Ogundele, O. F. Kayode, O. M., Ajaelu, C. J. (2017). Chemical and biological significance of naturally occurring additives on African black soap and its performance. *Journal of Applied Science in Environmental Management*, 21 (7): 1370-1373.
- [22] Ikotun, A. A., Coogan, M. P., Owoseni, A. A., Egharevba, G. O. (2019). Design, synthesis, physicochemical and antimicrobial properties of rhenium(I) tricarbonyl complexes of 3-(phenylimino)indole-2-one. *J. Chem Soc. Nigeria*, 44 (5): 948-958.
- [23] Shoukat, S., Bhatti, H.N., Iqbal, M., & Noreen, S.(2017). Mango stone biocomposite preparation and application for crystal violet adsorption: a mechanistic study. *Microporous Mesoporous Mater*, 239: 180-189
- [24] Thang, N. H., Khang, D. S., Hai, T. D. Nga., D. T., & Tuan, P. D. (2021). Methylene blue adsorption mechanism of activated carbon synthesized from cashew nut shells. *RSC Advance*, 11 : 26563-26570.
- [25] Hasan, S., & Güzel, F. (2015). "Performance of new mesoporous carbon sorbent prepared from grape industrial processing wastes for malachite green and congo red removal", *Chemical Engineering Research and Design*, 100: 27 – 38.
- [26] Varadwaj, G.B.B., Rana, S., Parida, K., Nayak, B.B. (2014). A multi-

- functionalized montmorillonite for co-operative catalysis in one-pot Henry reaction and water pollution remediation, *Journal of Material Chemistry, A* 2 (20) : 7526–7.
- [27] Khan, M. I. (2020). Adsorption of methylene blue onto natural Saudi Red Clay: isotherms, kinetics and thermodynamic studies. *Material Research Express*, 7: 055507
- [28] Lativa, J. M, Parushuram, Sangappa Y (2022). "Preparation, characterization, and methylene blue dye adsorption study of silk fibroin - graphene oxide nanocomposites", *Environmental Science: Advances*.
- [29] Ajaelu, C. J., Bamgbose, J. T, Atolaiye., B. O., & Adetoye A. A. (2008). The use of cyanomethemoglobin complex in estimating cyanogens potential of cassava and cassava products. *African. Journal of Biotechnology* 7 (10) : 1585-1587
- [30] Senthamarai, P. P., Kumar, S. M. P., Priyadharshini, V., Vijajalakshmi, V. P. ., Sivanesan, T. S. (2013). Adsorption behavior of methylene blue dye onto surface modified *Strychnos potatorum* seeds. *Environmental Progress and sustainable Energy*. 32(3): 624-632.
- [31] Bamgbose, J. T., Dare, E. O., Samuel, B. J., Ajaelu C. J. (2007). Swelling equilibrium and sorption kinetics of polyvinyl acetate film. *Journal of Chemical Society of Nigeria*. 32 (2) :144-150.
- [32] Dindorkara, S. S., Patel, R. V., & Yadav , A. (2022). Adsorptive removal of methylene blue dye from aqueous streams using photocatalytic CuBTC/ZnO chitosan composites, *Water Science Technology*, 85 (9) : 2748.
- [33] Cheng, J., Zhan, C., Wu, . J., Cui, . Z., Si, J., Wang, Q., Peng X., Turng, L.(2020). Highly Efficient Removal of Methylene Blue Dye from an Aqueous Solution Using Cellulose Acetate Nanofibrous Membranes Modified by Polydopamine. : *ACS Omega*, 5: 5389–5400.
- [34] Jan, S. U., Ahmad, Y., Ali, M. Hussain, Z., Melhi. S. (2021). “Adsorptive Removal of Methylene Blue from Aqueous Solution Using Sawdust”. *Medicon Pharmaceutical Science*, 2 (1) : 08-16.
- [35] Ajaelu., C.J. & Adetoye O. A (2023). Liquid phase adsorption of methylene blue on functionalized *Solanum macrocarpon* calyx activated carbon: kinetics, equilibrium, and thermodynamic studies. *International Journal of Environmental Science and Technology*. 1-12
- [36] Alao, O. Ajaelu, C. J., Ayeni. O. (2014). Kinetics, Equilibrium and Thermodynamic Studies of the Adsorption of Zinc on *Carica papaya* root powder. *Research Journal of Chemical Sciences*. 4(11), (2014) 1-6.